RSC Advances

REVIEW

View Article Online
View Journal | View Issue

Cite this: *RSC Adv.*, 2020, **10**, 42098

Non-ionic small amphiphile based nanostructures for biomedical applications

Badri Parshad,*[a] Suchita Prasad,[b] Sumati Bhatia,[c] Ayushi Mittal,[b] Yuanwei Pan,[c] Prashant Kumar Mishra,[d] Sunil K. Sharma[b] and Ljiljana Fruk*[a]

Received 22nd September 2020
Accepted 3rd November 2020

DOI: 10.1039/d0ra08092f

rsc.li/rsc-advances

Self-assembly of non-ionic amphiphilic architectures into nanostructures with defined size, shape and morphology has garnered substantial momentum in the recent years due to their extensive applications in biomedicine. The manifestation of a wide range of morphologies such as micelles, vesicles, fibers, tubes, and toroids is thought to be related to the structure of amphiphilic architectures, in particular, the choice of the hydrophilic and hydrophobic parts. In this review, we look at different types of non-ionic small amphiphilic architectures and the factors that influence their self-assembly into various nanostructures in aqueous medium. In particular, we focus on the explored structural parameters that guide the formation of various nanostructures, and the ways these structures can be used in applications ranging from drug delivery to cell imaging.

Amphiphiles and self-assembly

Self-assembly is a process by which atoms, molecules, or functional building blocks are joined together into well-defined hierarchic frameworks with structural versatility and often, with the ability to be modulated by external stimuli. Self-assembly has become a useful tool for the design of advanced functional nanomaterials over different length scales and with controlled morphologies, and it is driven by various non-covalent interactions such as hydrophobic, ionic, hydrogen bonding and π–π stacking. In fact, the life on Earth is very much driven by the self-assembly of molecular building blocks such as lipids, carbohydrates, proteins and nucleic acids, all of which generate structurally precise and functionally efficient supramolecular architectures.[1–5] The self-assembly process was first observed and described by Reinitzer in 1880s, during his study of organic soft matter, in particular, the exploration of the liquid crystal state, which allowed molecules to behave in a fluid-like manner due to the changes in weak intermolecular van der Waals force.[6] In synthetic chemistry, the self-assembly process has been brought into limelight after the failure of classical covalent organic synthesis to fabricate large structured aggregates with molecular complexity and adaptable activity found in biological macromolecules.[7] It was a driving force behind the development of supramolecular chemistry, and in the meanwhile, self-assembly strategies have driven advances in material design within the areas of physics, chemistry and nanotechnology.[8]

Among different classes of molecules used for preparation of biocompatible and tailor-made nanomaterials, the self-assembling behavior of small molecular amphiphiles has been extensively explored in the past decade. Characterized by dual binding affinity, the term amphiphile comes from the Greek roots: *αμφις*, *amphis*, for "both" and *φιλία*, *philia* for affinity, and was coined by Hartley in 1936.[9,10] The self-assembly of amphiphiles offers structurally precise and functional supramolecular architectures of distinct morphologies such as micelles, vesicles, fibers, tubes, toroids and others (Fig. 1). Assembly of these structures is a result solvophobic, or in particular, the hydrophobic effect within an aqueous environment aimed to achieve a state of minimum free energy and maximum stability.[11,12]

Amphiphiles and their ability to form supramolecular architectures by the interplay of hydrophobic and hydrophilic molecular domains has been initially exploited in the study and manufacture of soaps, fats and oils more than hundred years ago. Surfactants, compounds that lower the surface tension at the interface of two liquids, are typical amphiphilic molecules that have the capability to decrease the surface tension of a liquid or the interfacial tension between two liquids of different polarity, and are, therefore, widely used as detergents, dispersants, wetting agents, foaming agents and emulsifiers.[11] However, not all amphiphiles are surface active molecules and only those with almost equilibrated hydrophilic and hydrophobic tendencies are likely to migrate to the surface or interface. Phospholipids, which constitute the cell membranes, assemble in molecular bilayers by a process that is driven by a balanced volume ratio of water-exposed hydrophilic head groups and hydrophobic tails.

[a]*Department of Chemical Engineering and Biotechnology, University of Cambridge, Cambridge CB3 0AS, UK. E-mail: lf389@cam.ac.uk; bp448@cam.ac.uk*

[b]*Department of Chemistry, University of Delhi, Delhi 110 007, India*

[c]*Institut für Chemie und Biochemie, Freie Universität Berlin, Takustraße 3, 14195 Berlin, Germany*

[d]*School of Chemical and Process Engineering, University of Leeds, Leeds LS2 9JT, UK*

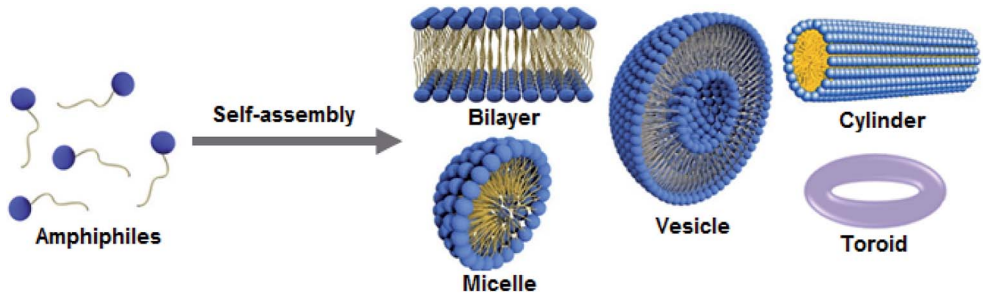

Fig. 1 Amphiphiles composed of hydrophobic tails and hydrophilic heads self-assemble into various shapes such as bilayers, micelles, vesicles, cylinders and toroids.

The continuous quest of researchers to mimic the natural self-assembled systems and increased need for functional materials for applications in drug delivery, bioimaging, environmental remediation and surface coating, has prompted design of synthetic amphiphiles. Harnessing the potential of self-assemblies of amphiphiles entails playing with the experimental variables together with the engineering of their functional, structural and chemical properties.

Within this review, we discuss the chemical structure of different types of small non-ionic amphiphiles, and give an overview of the assembled structures and their transport applications. There have been numerous publications that address small non-ionic amphiphiles. Herein, we review mainly different types of polyethylene glycol (PEG, Fig. 2) and polyglycerol (PG, Fig. 2) based small non-ionic amphiphiles. The addition of PEG to pharmaceutical formulations has several advantages such as increased water solubility and renal clearance, high chemical stability, decreased interaction with blood components and improved biocompatibility.[13] Use of PEG also results in the formation of stable micelles with a buffer layer, which minimizes unfavorable interactions of the micelles with proteins, enzymes and cells. Such ability is known as 'stealth' property, and has been used to make more efficient nanoscale delivery vesicles, and successful drug formulations including Oncaspar, Adagen, Pegasys, Neulasta and Caelyx.[14] On the other hand, polyglycerol (PG) belongs to a class of oligoethers and has a biocompatibility profile similar to PEG, and has emerged as a potential alternative to PEG.[15] PG dendrons possess a compact, well-defined dendrimer-like architecture but unlike dendrimers, PG dendrons do not exhibit clearly distinguishable interior or periphery, and possess two types (primary and secondary) of hydroxyl functionalities (Fig. 2). Employing the "selective chemical differentiation" strategy for modification of these hydroxyl groups enables to generate versatile architectures using a PG scaffold.[16]

Besides giving the overview of different types of small non-ionic amphiphiles, we explore morphological aspects of amphiphilic architectures and their applications. Finally, we conclude with remarks on the recent developments, lessons learned and the future applications. For detailed account of other types of amphiphiles such as polymeric, dendritic and small ionic ones, we recommend review articles by Sorrenti *et al.*,[11] Rosen *et al.*,[17] Thota *et al.*,[18] and Parmar *et al.*[19,20]

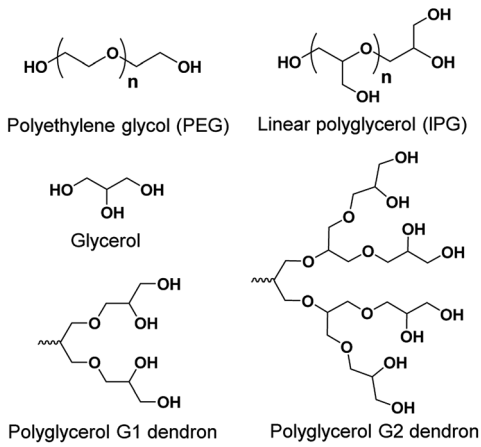

Fig. 2 Structures of polyethylene glycol (PEG) and linear polyglycerol (lPG) and polyglycerol dendrons. Depending upon the pattern and number of glycerol units, we distinguish PG G1 dendron (2 PG unit), G2 (4 PG units) and larger PG Gx.

Morphological aspects of amphiphile assembly

Among the various interactions such as hydrogen bonding, van der Waals forces, π–π stacking, metal-ion, electrostatic and hydrophobic interactions responsible for the self-assembly, the self-assembly of non-ionic amphiphiles is predominantly governed by hydrophobic interactions. In a nutshell, the hydrophobic moieties assemble in order to minimize the contact with polar solvent molecules, which results in intramolecular distribution of lipophilic and hydrophilic segments. Despite the weak hydrophobic interactions involved in self-assembly, the high number of these weak forces results in stable self-assembled structures in aqueous environment.[21] A model-based theory developed by Israellachvili *et al.* elucidates the morphology of the architectures by examining the geometry of individual molecules.[22,23] According to this theory, the nanostructure of amphiphilc aggregates formed in aqueous solution can be predicted by calculating the packing of the amphiphile characterized by critical packing parameter (p).

$$p = v/a_0 l_c$$

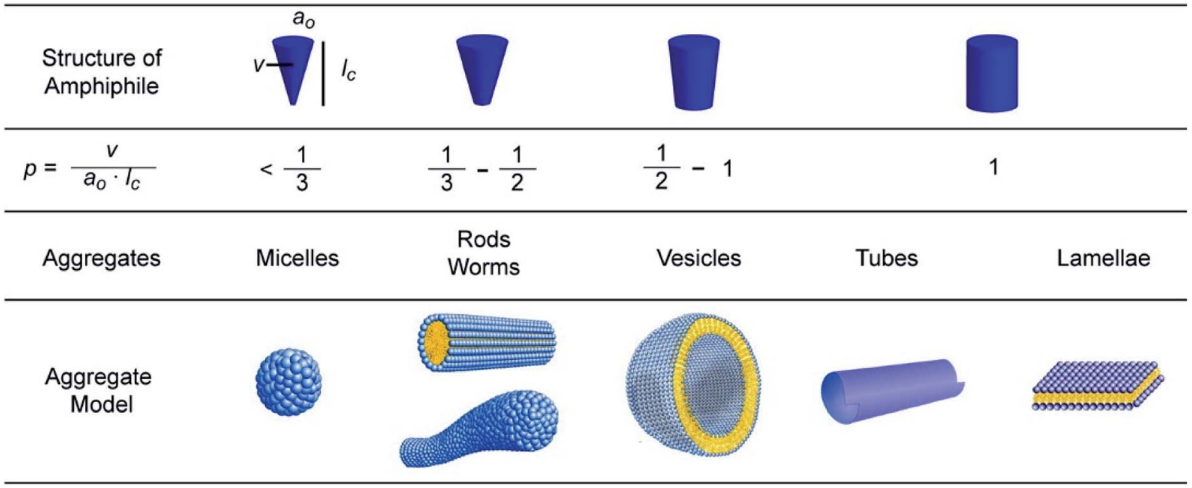

Fig. 3 Influence of the packing parameter (p) of an amphiphile on the morphology of the nanostructure. Reprinted with permission from ref. 18. Copyright 2016 American Chemical Society.

where, v is the effective volume occupied by the hydrophobic portion in the core, a_0 is the equilibrium area of the hydrophilic surface group, *and* l_c is the maximum effective chain length of the individual amphiphile.

Depending on the p value, the aggregates can be micellar ($p \leq 1/3$), cylindrical ($1/3 \leq p \leq 1/2$), in form of vesicles ($1/2 \leq p \leq 1$), or lamellar ($p = 1$) as depicted in Fig. 3.

Micelles

Micelles are small, self-assembled and thermodynamically stable nanostructures with inner hydrophobic cores formed by the amphiphile tails, which is shielded from water by a corona constructed from hydrophilic head groups. An archetype for self-assembly of surfactants or lipid amphiphiles, micellization is a spontaneous process occurring above a certain amphiphilic concentration known as critical micelle concentration (CMC) and at temperatures above the Krafft temperature (the minimum temperature at which aggregation occurs).

Formation of micelles can be explained by the thermodynamics of the process. The enthalpic and entropic contributions ensue from energetically favorable interactions between the hydrophobic skeletons of amphiphiles (enthalpic) and the local distribution of water molecules due to hydrogen bonding (entropic). The hydrogen bonds between water molecules are interrupted by the segregated amphiphilic hydrocarbon chains leading to entropically unfavorable ordered structure. In order to evade the disruption of water distribution and re-establish the hydrogen bond network, micelle formation occurs as it is entropically more favorable than the isolated amphiphilic molecules. Formation of ordered structures helps in the reduction of free energy of the system by eliminating hydrophobic groups from direct contact with water and can be regarded as an alternative mechanism to adsorption at the interfaces.

Vesicles

Vesicles, spherical or ellipsoidal closed amphiphile structures with an internal cavity containing the aqueous solution, have gained lots of attention in drug delivery, pharmaceutical formulations, cosmetics and material architectonics.[24–30] Unlike micelles, vesicles contain a bilayer coat. The most prominent vesicle structures used in drug delivery are liposomes formed from the membrane-like phospholipid bilayer. Liposome loaded with the chemotherapeutic drug doxorubicin, known as Doxil has been used in treatment for various cancers since 1995.[31]

Although, in general, vesicles have characteristic sizes ranging from 10–100 nm, there have been some as big as several hundreds of nanometers to several micrometers. Unilamellar vesicle is a conventional vesicle formed from a single bilayer structure comprising of two monolayers with their hydrophobic parts facing each other, whereas onion-like structure containing multilayer vesicles result from multiple concentric bilayer surfaces (Fig. 4). Vesicles are of great importance in biomedical field because they can be employed as carriers for the delivery of both hydrophobic and hydrophilic dyes/drugs.

Other self-assemblies

Apart from micelles and vesicles, formation of diverse self-assembled architectures is possible through subtle structural changes and modulation of concentration, surfactant geometry, and other experimental variables such as temperature, pH and ionic strength. Fibers, tapes, toroids, and tubes are other self-

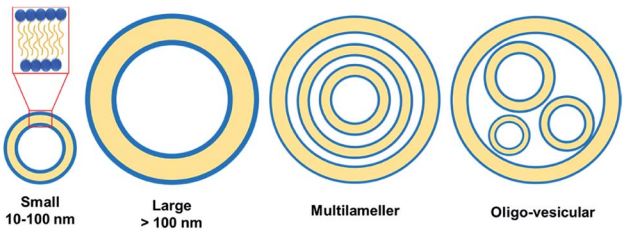

Fig. 4 Structural representation of different types of vesicles: small unilamellar, large unilamellar, multilamellar (onion like layered lamellae) and oligo-vesicular (small vesicles incorporated into a bigger one) vesicles.

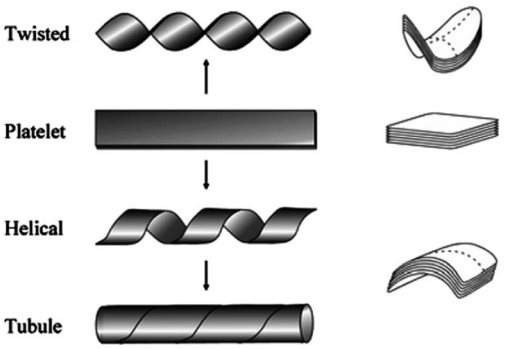

Fig. 5 Transformation of Platelet structure into twisted ribbon, helical and tubule structures. Reprinted with permission from ref. 33. Copyright 2007 American Chemical Society.

assemblies that require special directional interactions between the amphiphiles alongside the hydrophobic interactions to afford the self-assembly in a specific direction.[32] For example, such directional assembly can be achieved by aromatic interaction through π–π stacking in water. Micellar fibers are the simplest supramolecular aggregates that possess high aspect ratio making them long and narrow. They consist of material filled cylinders with the diameter of a molecular bilayer or a single molecule length if formed by a single head/tail amphiphiles or bolaamphiphiles, respectively. Ribbons are fibrous aggregates based on distorted bilayers. The ribbon-based aggregates have been morphologically classified into: (a) helical and tubular structures, displaying a cylindrical curvature, and (b) twisted ribbons with a Gaussian or saddle-like curvature.[33] In fact, experimental evidence on different systems has shown an intimate relationship between helical ribbons and tubules (Fig. 5).

Helices can serve as precursors of tubules under certain conditions. Shortening of the helical pitch of the ribbon at a constant tape width, and widening of the tape width at a constant helical pitch have been reported as the two mechanisms for the nanotube formation from helical ribbons. It has been observed that both helices and tubes exist in solution only at temperatures below the gel-to-liquid crystalline phase transition temperature (T_{g-l}) of the amphiphile. At temperature higher than T_{g-l}, the morphology changes to vesicles. These have high aspect ratio and large curvature, and are usually formed by less soluble amphiphiles. Toroids possess a unique annular shape with an internal pore in the central region resembling a short nanotube with a length of few nanometers, and commonly formed of transmembrane proteins.[34] The morphological properties of amphiphiles are of huge importance for various biomedical applications, in which the size and CMC are of utmost significance.

Types of amphiphiles, amphiphile-guided nanostructures and their biomedical applications

Amphiphilic architectures can be classified as polymeric and non-polymeric, of which non-polymeric small amphiphiles have gained considerable attention owing to their precise control over molecular weight, hydrophobic–hydrophilic balance, and well-defined and reproducible structures. The chemical nature of the polar head, the charge of the head group, and the number and type of bonding between polar head(s)/hydrophobic tail(s) are some of the criteria that have been employed for the classification of amphiphiles.

According to the head group charge, they have been classified as ionic or non-ionic (Fig. 6), however, the latter have emerged as potential biomedical candidates due to the limitations posed by the ionic counterparts. Namely, non-ionic amphiphiles are characterized by the pH-independent self-assembling behavior, biocompatibility and skin tolerance, which makes them desirable for use in cosmetics and medicine. On the other hand, ionic amphiphiles exhibit challenging toxicity profile and may show undesired ionic interaction with biomolecules inside biological system. The positive charge within cationic amphiphiles favor non-specific interactions with negatively charged serum albumine protein, low density lipoproteins and macroglobulins, and myriads of other negatively charged biomolecules.[35–37] These undesired electrostatic interactions lead to undesired deactivation of biomolecular species, and have even been shown to promote the binding of amphiphile complex to the surface of the cells and other biomolecules compromising their inherent activity and increasing the toxic response.[38] Anionic amphiphiles might also exhibit undesirable toxicological profile due to their persistence inside the cells after the delivery of therapeutic molecules. In addition, they can also engage in unfavorable interaction with positively charged metal ions within the biological system.

On the basis of the number and kind of connection of polar head(s)/hydrophobic tail(s), amphiphiles are categorized as conventional *linear* or single head/single tail amphiphiles attached to each other in linear fashion, *bolaamphiphiles* composed of two hydrophilic heads connected by a hydrophobic skeleton, *dimeric amphiphiles* containing two hydrocarbon tails and two hydrophilic groups linked by a spacer, and *dendritic amphiphiles* (Fig. 7).

Linear amphiphiles

In a conventional linear amphiphile, hydrophobic and hydrophilic parts are attached to each other in linear fashion. This is the simplest form of amphiphile consisting of one hydrophilic

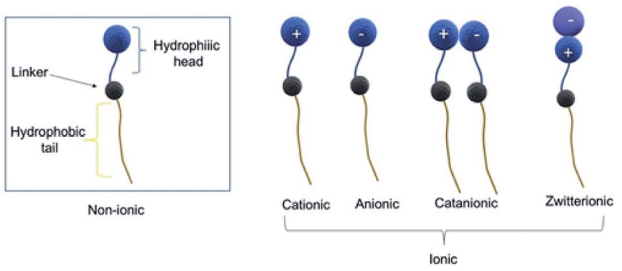

Fig. 6 Based on their charge amphiphiles can be classified into non-ionic and ionic. Different subclasses of ionic amphiphiles are shown.

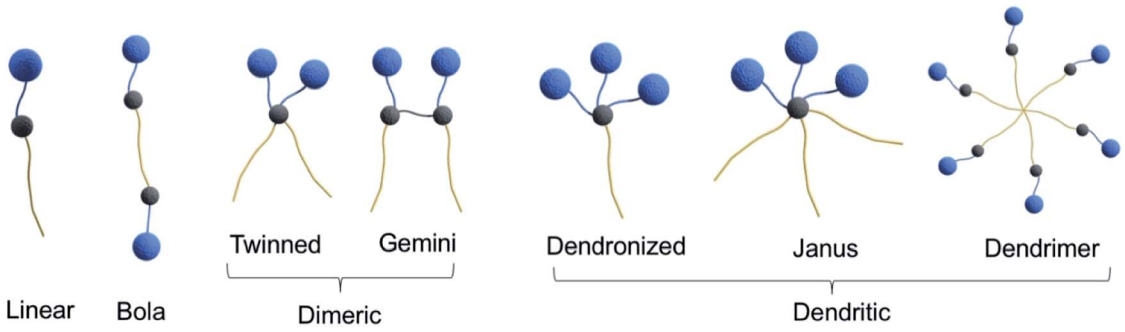

Fig. 7 Classification of amphiphiles based on their structure.

and one hydrophobic part and capable of aggregation in aqueous environment. These type of non-ionic amphiphiles are less common because of high critical aggregation concentration and low miceller stability. A large variety of simple non-ionic amphiphiles consisting of hydrophilic PEG unit linked to hydrophobic alkyl chain (Fig. 8), such as Brij surfactant (C_nEO_m *e.g.* $\mathbf{C_{18}EO_{20}}$ and $\mathbf{C_{18}EO_{100}}$), are used for enhancing the solubility of poorly water soluble drugs.[39] Moreover, surfactant $\mathbf{C_{12}EO_7}$ along with ionic surfactants is used in cleaning applications as domestic detergent such as laundry cleaning products.

Bolaamphiphiles

Bolaamphiphiles, also known as bolaphiles or bolaform surfactants, are a novel class of amphiphiles exhibiting a hydrophobic framework which may be one, two or three alkyl chains, a porphyrin or a steroid, flanked by hydrophilic segments. The name originates from the word 'bola' which stands for an old South American weapon formed from a long cord or thong with heavy metal balls at the end and employed for throwing at and entangling cattle. Originally, 'bolaform electrolyte' was a term coined by Fuoss and Edelson for a hydrophobic skeleton linking two ionic head groups.[40] Compared to mono-polar amphiphiles, the introduction of a second hydrophilic group confers higher water solubility and reduced critical aggregation concentration, and the membranes composed of these architectures have lesser permeability and higher durability. They were first discovered within the membranes of extremophile archaea in the early 1980s.[41,42] The archaeal cytoplasmic membrane contains unique ether lipids that cannot be easily degraded, are temperature and mechanical resistant and highly salt tolerant. Moreover, thermophilic and extreme acidophilic archaea possess membrane-spanning tetraether lipids that form a rigid monolayer membrane which is nearly impermeable to ions. These properties make the archaeal lipid membranes more suitable for life in extreme environments than the ester bilayer lipids of bacteria and eukarya.

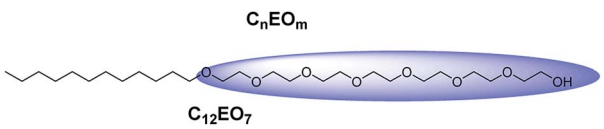

Fig. 8 Examples of commonly used non-ionic PEG-based amphiphilic molecule, where C is alkyl chain carbon atom and EO is ethylene oxide unit.

Significant number of self-assembled architectures has been formed from bola amphiphiles. This is mainly ascribed to their structural similarity to A–B–A type triblock copolymers, which permits versatile modification and structural rearrangements. For example, aggregation can be affected through the variation of both the structure of the head groups and that of the spacers, which is usually not possible in case of simple conventional surfactant systems.

However, the isolation technique of bolaamphiphiles from natural sources constrained their investigation, thus, pushing the researchers towards chemical synthesis to design mimics of natural amphiphiles. For example, a series of ester linkage containing bolaamphiphiles has been reported, which were synthesized *via* a chemo-enzymatic approach using an immobilized enzyme (lipase) from *Candida antarctica* (Novozym 435) and employing biocompatible starting materials *such as p*-hydroxybenzoic acid, *m*PEG, and glycerol (Fig. 9).[43] Triazole rings or amides were used to functionalize the hydrophobic segments in pursuit of the comparative study between these two functionalities. In an attempt to attain enhanced stability of supramolecular assemblies and solubility of hydrophobic guest molecules, aromatic unit was introduced. The synthesized amphiphiles were studied for their self-assembly and encapsulation behavior using different drugs/dyes in aqueous medium. Cryo-TEM technique was used to evaluate the aggregation behavior of compounds **1a** and **1b**.The micrograph of compound **1b** depicts the formation of globular and thread-like micelles in the range of 5 nm diameter, while compound **1a** assembled into small globular micelles of size < 4 nm. Further, no significant change in size was observed after the encapsulation of desired molecules. The study of the enzyme-responsive behavior of the synthesized bolaamphiphiles using a hydrolase enzyme demonstrated that amide based nanocarriers disassembled and released the encapsulated cargo on incubation with the enzyme.

Synthesis, encapsulation, and cellular uptake of PEG and PG based bolaamphiphiles have also been reported recently (Fig. 10).[44] Amphiphiles **2a** and **2c** displayed higher transport potential of nile red in comparison to their larger analogues *i.e.*

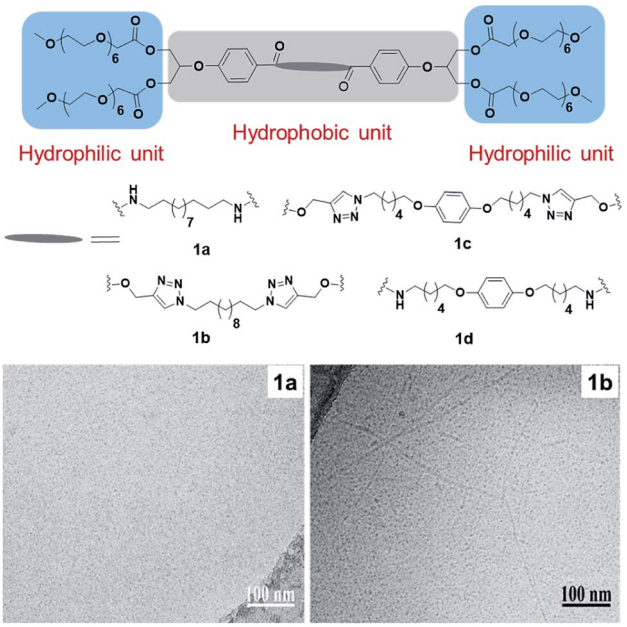

Fig. 9 Structures of bolamphiphiles (**1a–1d**) and cryo-TEM images of amphiphiles **1a** and **1b**. Small globular micelles can be observed in image **1a**, and elongated thread-like micelles in **1b**. Reprinted with permission from ref. 43. Copyright 2018 Elsevier.

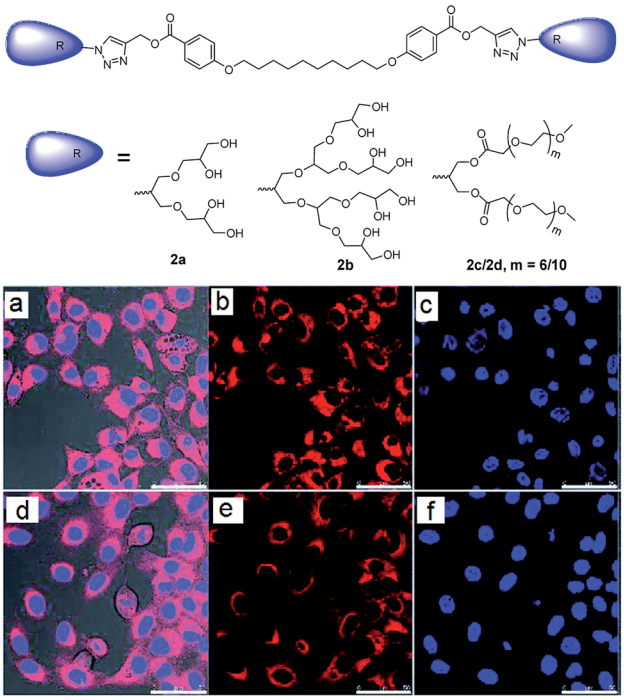

Fig. 10 Molecular structures of bolaamphiphiles (**2a–2d**), which were used to encapsulate nile red dye and deliver it into cells and CLSM images of A549 cells after 24 h of incubation with nile red encapsulated amphiphiles **2c** (a–c) and **2a** (d–f). Adapted with permission from ref. 44. Copyright 2018 Royal Society of Chemistry.

2b and **2d**, respectively. Enzyme mediated release of the cargo was also studied by using lipase (Novozym 435), which showed the complete release from **2c** within 5 hours. Confocal laser scanning microscopy of nile red encapsulated **2a** and **2c** showed that both the studied amphiphiles exhibited a similar dye uptake pattern inside the cell. After 24 h, more dye accumulation was observed inside the cytosol. This proved that the amphiphilic nanocarriers were capable of delivering nile red into the cytosol of cells (Fig. 10). Cytotoxicity profile showed that the amphiphiles were well tolerated up to 0.5 mg mL^{-1} by A549 cells.

Wyszogrodzka *et al.* reported the synthesis of dendron based triblock amphiphiles in order to improve the solubility of hydrophobic entities, with nile red chosen as a model compound.[45] Each of the amphiphile consisted of hydrophobic biphenyl core and hydrophilic PG dendron surface (Fig. 11). They found that the amount of nile red encapsulated in these amphiphiles decreased with an increase in dendron generation, an opposite trend than the expected. This behavior was explained by assuming the formation of amphiphilic aggregates instead of unimolecular transport behavior. In one of their other approaches to solubilize nile red, a similar type of water soluble compound consisting of aromatic core was synthesized by using diethylenebenzene and monoazide G1/G2/G3 dendron *via* click chemistry.[46] The structure-transport relation of these dendrimers clearly showed that the amount of nile red encapsulated was dependent upon the dendron generation present at the surface.

Azobenzene-based bolaamphiphiles synthesized by Urner *et al.* were studied for water solubility by analyzing the structure, flexibility and *cis–trans* isomerization of the hydrophobic backbone of the amphiphiles (Fig. 10).[47] Irradiation at 365 nm causes *trans* to *cis* isomerization, while *cis* to *trans* isomerization is a result of thermal equilibrium and/or irradiation at 490 nm. These light-induced changes were shown to affect the water solubility of amphiphiles, which did not only depend on the hydrophobic-hydrophilic balance, but also by flexibility of the system. The solubility of different amphiphiles before and after irradiation with 365 nm wavelength is shown in Fig. 12b. Lower solubility was observed for rigid and short linker containing *trans*-bolaamphiphile **4a**, but increased significantly after irradiation at 365 nm. On the hand, bolaamphiphile **4a*** which contains a flexible linker showed higher solubility even in the absence of light.

In the earlier study by the same authors, ion mobility-mass spectrometry (IM-MS) was employed to complement the UV-Vis data and monitor the *cis–trans* isomerization of bolaamphiphile **4c**.[48] In addition, TEM analysis was employed to study the structures formed, which revealed that *trans*-isomer of compound **4c** resulted in twisted tapes with thickness of 5 nm and width of approximately 20 nm, which were destroyed by 366 nm irradiation (Fig. 13).

Such an ability to control the structure by external stimuli such as light is a desirable feature of nanostructure design, and might be useful for design of responsive drug delivery systems.

Twin or dimeric amphiphiles

Twin or dimeric amphiphiles have been known in patent literature for a long time, however, the first paper on their synthesis was published by Bunton *et al.* in 1971, who described the

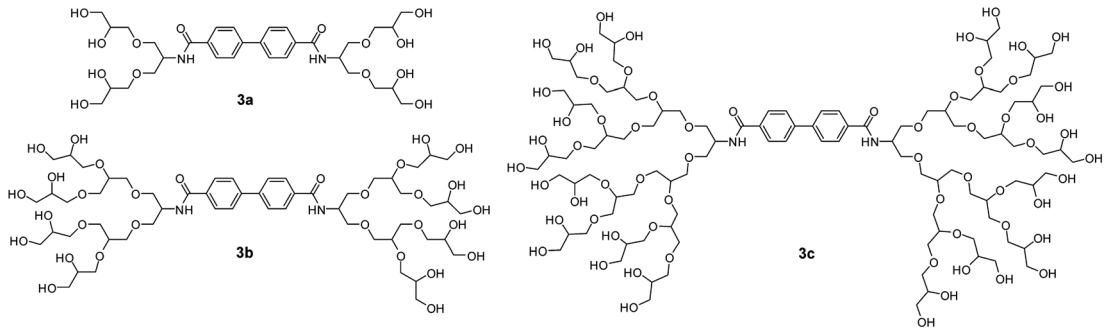

Fig. 11 Molecular structures of triblockamphiphiles (**3a–3c**) used to designed transport vehicles for nile red. Adapted from ref. 45.

preparation of quaternary ammonium bromide dimeric surfactants.[49] This was followed by development of various bis-quaternary ammonium and anionic dimeric surfactants,[50,51] and the introduction of the term "Gemini surfactant" by Menger and Littau in 1991 to describe this class of super active second generation surfactants.[52] Due to the presence of two hydrophobic tails and two hydrophilic head groups linked by a flexible or rigid spacer at the level of or in close vicinity to the head groups, geminis have excellent self-assembly properties suitable for design of complex architectures.[53–55] In addition, they possess superior physiochemical properties such as low CMC, high solubilization capacity due to presence of two hydrophilic groups, high surface activity, low Krafft temperature, and multiple aggregate morphologies, compared to the conventional monomeric surfactants.[56,57] Owing to these properties, they have shown great promise as long circulating drug carriers, skin and body care products, and oil recovery, among others.

The synthesis of twinned amphiphiles using A_2B_2 spacer, as well as the investigation of the influence of the length of both the PEG moiety and hydrophobic alkyl chain on the formation and aggregation of nanostructures was reported by Singh *et al.* (Fig. 14).[58] Depending on the amphiphile's molecular structure, globular, thread-like micelles and planar double-layer assemblies in accordance with Israelachvili's packing parameter model were observed by cryo-TEM measurements. Amphiphile **5a** having relatively large hydrophobic part and short hydrophilic PEG chain resulted into planar bilayer ribbon-like aggregates. On the other hand, amphiphile **5d** with short hydrophobic part and long hydrophilic PEG chain resembled cone-shaped geometry and formed globular micelles. Contrary to this, amphiphiles **5c** having long PEG chain/long hydrophobic part and **5b** short PEG chain/short hydrophobic part, exhibited slightly cone-shaped geometry and self-assembled to form rod-like nanostructures with diameter 8.5 nm and 5.0 nm, respectively. In order to demonstrate their applicability as nanocarriers, encapsulation studies of hydrophobic drug nimodipine, a calcium channel blocker originally developed for the treatment of high blood pressure and bleeding in the brain, was carried out using the amphiphiles **5b**, **5c** and **5d**. Cytotoxicity study carried out for amphiphiles **5b**, **5c** and **5d** revealed that the amphiphiles were well-tolerated up to a concentration of 0.1 mg mL^{-1}. In addition, even an extended incubation for up to 3 days did not result in an increased toxicity, thus, suggesting that they are suitable for *in vivo* applications. However, it should be noted, that 2D cell studies are not necessary representative of the *in vivo* systems, and more advanced studies employing 3D organoid and spheroid studies should be introduced into the testing workflow to ensure the success of *in vivo* studies.

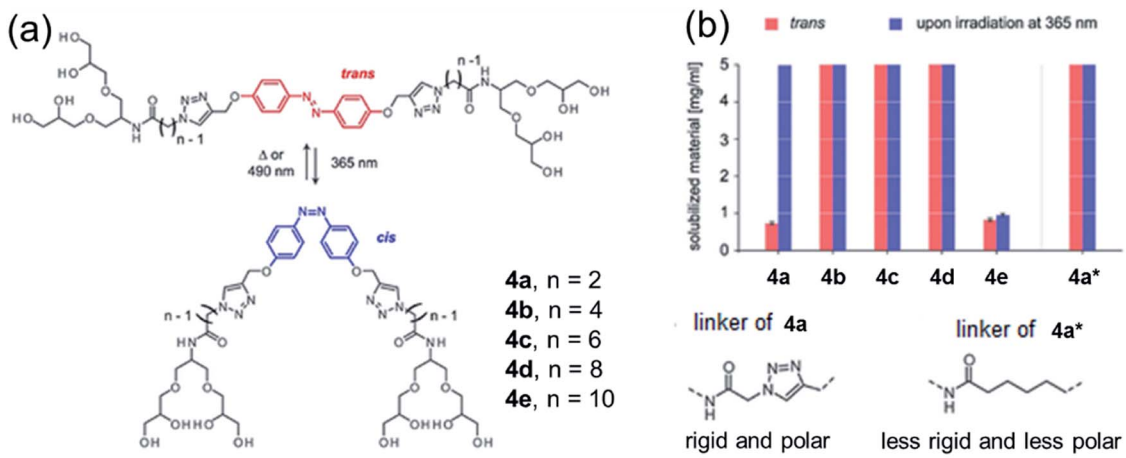

Fig. 12 (a) *Cis–trans* isomerization of azo-benzene modified bolaamphiphiles, and (b) water solubility of amphiphiles before and after irradiation at 365 nm. Less rigid linkers such as those shown **4a*** are soluble even in the absence of light, while rigid linkers require irradiation. Adapted with permission from ref. 47. Copyright 2019 Wiley-VCH Verlag GmbH & Co. KGaA.

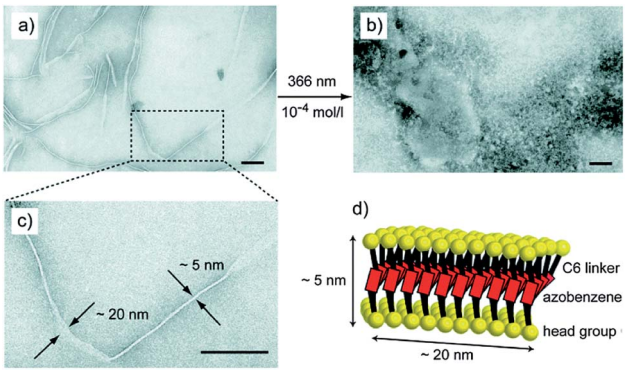

Fig. 13 Transmission electron micrographs (TEM) of aggregates formed by amphiphile **4c**; (a, c) twisted tapes of width of 20 nm and thickness of 5 nm are formed by *trans* isomer, (b) amorphous structures are observed upon irradiation indicating that the regular structure is destroyed and (d) schematic model of *trans* **4c** showing the formation of twisted tapes. Reprinted with permission from ref. 48. Copyright 2015 Royal Society of Chemistry.

Prasad *et al.* reported the synthesis of non-ionic dimeric amphiphilic constructs fashioned with suitable functionalities using 2,2-di(prop-2-yn-1-yl)propane-1,3-diol as the core unit (Fig. 15). The diol was successfully grafted with alkyl chains of variable lengths (C_{10}/C_{18}) and *m*PEG (M_n: 550/1000 g mol^{-1}) to confer hydrophobicity and hydrophilicity, respectively.[59] Nano-sized species generated from PEGylated amphiphiles exhibited DLS size ranging from 6–19 nm and formed micellar assemblies

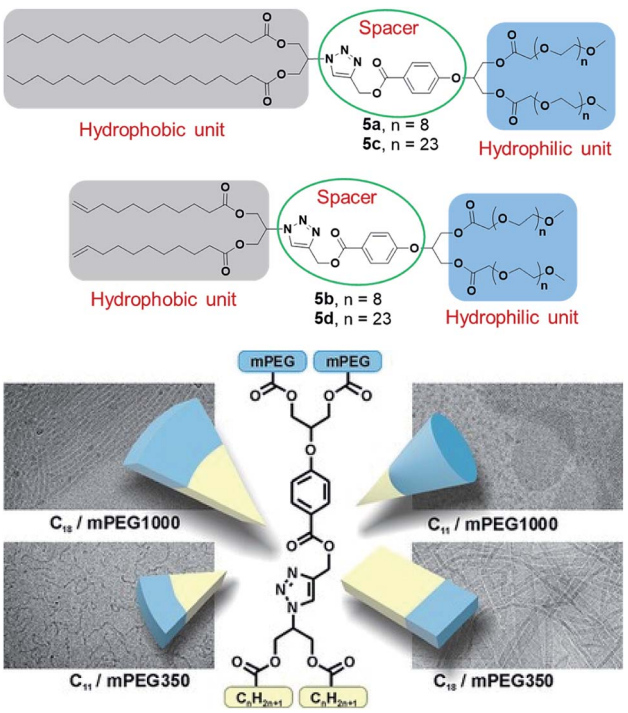

Fig. 14 Structures of twinned amphiphiles (**5a–5d**) and geometry of amphiphiles along with cryo-TEM images of formed aggregates. Reprinted with permission from ref. 58. Copyright 2017 Wiley-VCH Verlag GmbH & Co. KGaA.

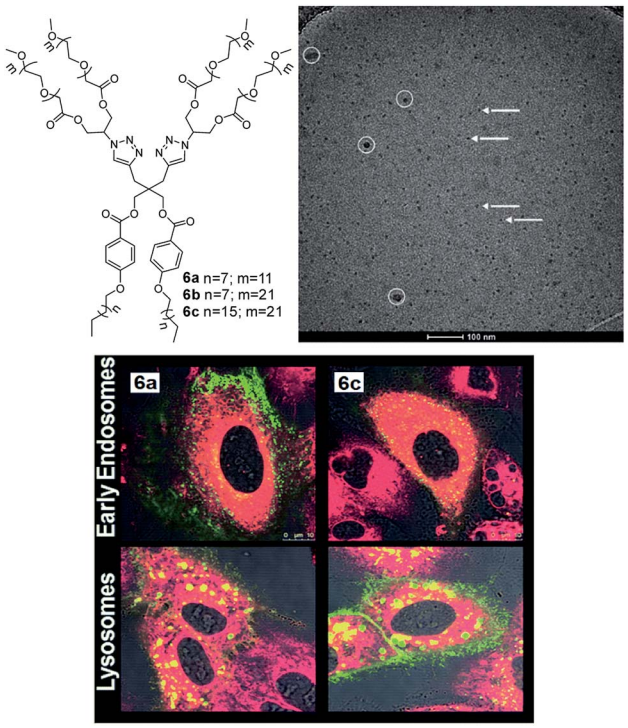

Fig. 15 Molecular structures of gemini amphiphiles **6a–6c** and cryo-TEM image of amphiphile **6c** displaying micelles shown by arrows. White circles indicate the surface contamination. Adapted from ref. 59. Copyright 2017 Royal Society of Chemistry.

confirmed by cryo-TEM study. The solubilization behavior of mPEG based amphiphilic nanocarriers (**6a–6c**) suggested the effective encapsulation of model hydrophobic species nimodipine, curcumin, dexamethasone and nile red. In pursuit of

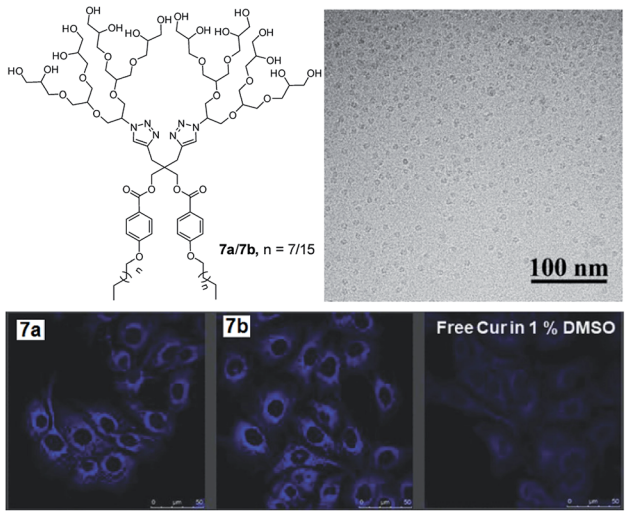

Fig. 16 Structure of the non-ionic amphiphiles **7a** ($n = 7$) and **7b** ($n = 15$) composed of alkyl and PEG chains. Cryo-TEM image of the aqueous solution of amphiphile **7b** shows globular micelles with a uniform diameter of 7.4 ± 0.6 nm. CLSM images of A549 cells after 4 h incubation with curcumin encapsulated amphiphiles. Adapted with permission from ref. 63. Copyright 2018 Wiley-VCH Verlag GmbH & Co. KGaA.

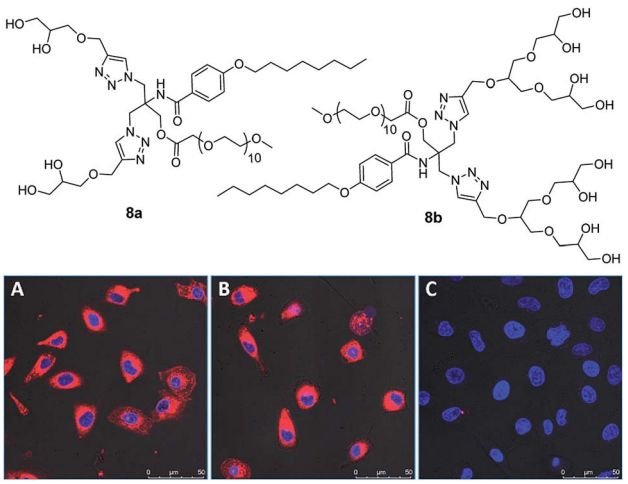

Fig. 17 Molecular structures of amphiphiles **8a** and **8b** studied for encapsulation of curcumin, dexamethasone and nile red. CLSM images of A549 cells incubated with amphiphile **8b** encapsulated with nile red after 4 h (A) and 24 h (B). Non-treated cells (C) have been used as a control showing blue-stained nucleus. Nile red is shown in red. Adapted from ref. 62. Copyright 2020 Elsevier.

a comparative study of the synthesized amphiphiles with a standard excipient, Cremophor® ELP was used, wherein absorbance spectra measurements revealed that the developed systems had higher or equivalent solubilization for curcumin. Cellular uptake experiment for studying cellular internalization of nile red encapsulated in two selected amphiphiles **6a** and **6c** in A549 lung cancer cells was carried out by confocal laser scanning microscopy (Fig. 15). The study demonstrated that efficient uptake of encapsulated dye in the cytosol and lysosomes of lung cancer cells occurred, indicating that the amphiphilic systems can transport drugs into cells. Furthermore, the cytotoxicity profile obtained from MTS assay unraveled that the synthesized amphiphiles exhibited negligible cytotoxicity at the tested concentrations (2, 1, 0.5 and 0.1 mg mL^{-1}), which is relevant for drug delivery systems. The enzyme-triggered release study revealed that amphiphile **6c** was susceptible to enzymatic decay as indicated by decrease in fluorescence intensity with time.

Dendritic amphiphiles

Dendritic amphiphiles, lying at the interface of classical amphiphiles and amphiphilic polymers in terms of structure and self-assembly, are characterized by a high degree of branching and multiple functionalities at the surface. These properties are described by their name which stems from a Greek word 'dendron' meaning 'tree'. In comparison to mono-polar amphiphiles, the self-assembled structures formed by the dendritic amphiphiles are more stable, as multiple branching provides them with enough density to circumvent inverse micellization by inverting the branches. For this reason, this class of amphiphiles has been particularly well suited for design of nanostructures for biomedical applications.

Sharma *et al.* reported different types of non-ionic dendritic architectures for drug delivery applications.[60–62] In one of their work, they reported small non-ionic dendritic amphiphiles (**7a** and **7b**) possessing polyglycerol G2 dendron as hydrophilic unit and C_{10} and C_{18} alkyl chains as hydrophobic tails.[63] These amphiphiles exhibited low CMC in the order of 10^{-5} M and hydrodynamic diameters in the range of 8–10 nm, with the nano-transporters **7a** and **7b** possessing the highest

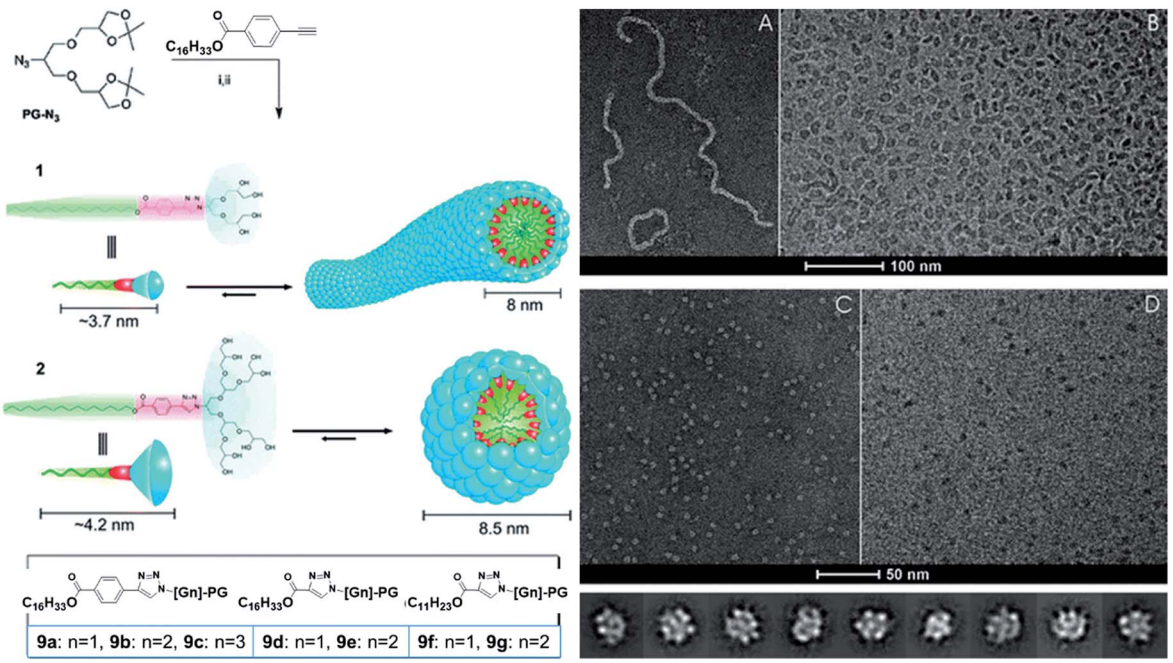

Fig. 18 Dendron amphiphiles and their self-assembly. (A) Cryo-negative stain (A) and cryo-TEM image (B) of aqueous solutions of amphiphile **9a**, and cryo-negative stain (C) and cryo-TEM image (D) of aqueous solutions of amphiphile **9b**. Adapted with permission from ref. 65. Copyright 2010 American Chemical Society.

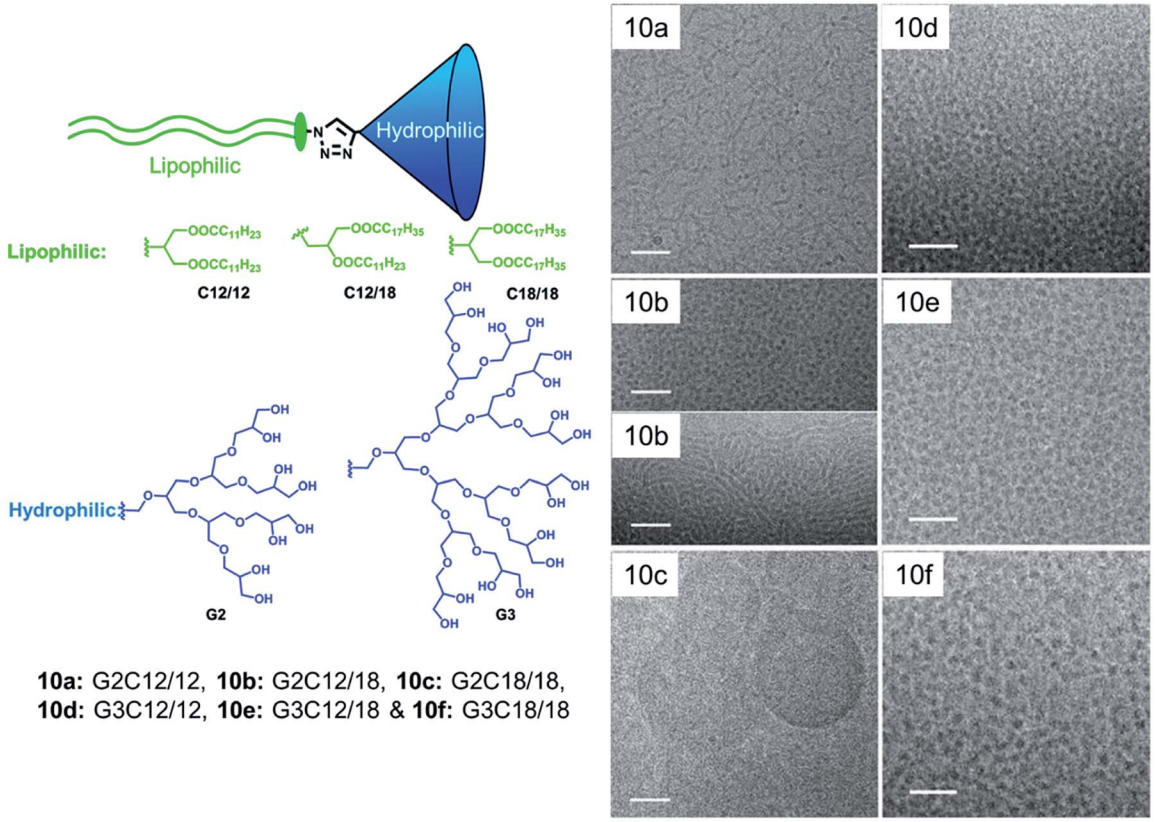

Fig. 19 Structures of dendron amphiphiles (**10a–10g**) and cryo-TEM image of aqueous solutions of amphiphiles where the left column scale bar is 50 nm and the right column scale bar is 30 nm. Adapted from ref. 66. Copyright 2010 Royal Society of Chemistry.

encapsulation efficiency of 80.74 and 98.03% for curcumin. Cryo-TEM image of the aqueous solution of amphiphile **7b** showed the formation of globular micelles with a uniform diameter of 7.4 ± 0.6 nm (Fig. 16). Efficient uptake of encapsulated curcumin in adenocarcinoma human alveolar basal epithelial (A549) cells was demonstrated by confocal laser scanning microscopy (Fig. 16). Amphiphiles **7a** and **7b** were found to be non-cytotoxic towards at studied concentrations with more than 80% cell viability observed up to the concentration of 1.0 mg mL^{-1}. However, encapsulated curcumin samples reduced the viability of A549 cancer cells *in vitro* more efficiently compared to free curcumin, which suggested the enhanced anticancer effect of amphiphile formulated curcumin.

In another report by the same research group, novel class of non-ionic amphiphiles were synthesized using a combination of polyethylene glycol and oligoglycerol dendrons as hydrophilic units alongside the alkoxy aryl moiety as hydrophobic unit.[62] The resulting amphiphiles aggregated in aqueous medium as confirmed by DLS and cryo-TEM studies, with particle size varying from 6 to 12 nm. Moreover, efficient encapsulation of nile red, curcumin and dexamethasone was observed in the interior hydrophobic cavity of the synthesized amphiphilic architectures. Cytotoxicity studies revealed that amphiphile **8b** constituting triglycerol unit was more cytocompatible as compared to other synthesized amphiphiles. Cellular uptake study demonstrated that nile red encapsulated in amphiphile **8b** internalized in A549 cells, with an increase in fluorescence intensity after 24 h, indicating the continuous uptake of the dye into the cytosol of the cells. The biomedical application of synthesized amphiphiles was further investigated for dermal drug delivery on excised human skin using nile red encapsulated in the nanocarrier **8b**, wherein an increased penetration of nile red to the viable epidermis and dermis layers of the skin was found even after 6 h. The release profile of drug/dye encapsulated amphiphile **8b** was studied under physiochemical conditions in the presence of immobilized lipase Novozym 435 that demonstrated time-dependent decay of the amphiphile and the release of the trapped cargo.

A novel-class of triglycerol based hydrolase responsive amphiphilic architectures were synthesized by using PEG as hydrophilic unit and alkyl chain (C_{15} and C_{18}) as hydrophobic part, and employing chemo-enzymatic approach.[64] Fluorescence measurements and DLS studies showed that all the amphiphiles self-assembled in aqueous medium with low CAC in the order of 10^{-5} M and DLS size in the range of 8–10 nm. Among all, amphiphiles having higher HLB value encapsulated the highest amount of drug nimodipine and dye nile red. Enzyme triggered release were also studied for the synthesized amphiphiles using nile red, which showed the release of around 90% dye within 72 h.

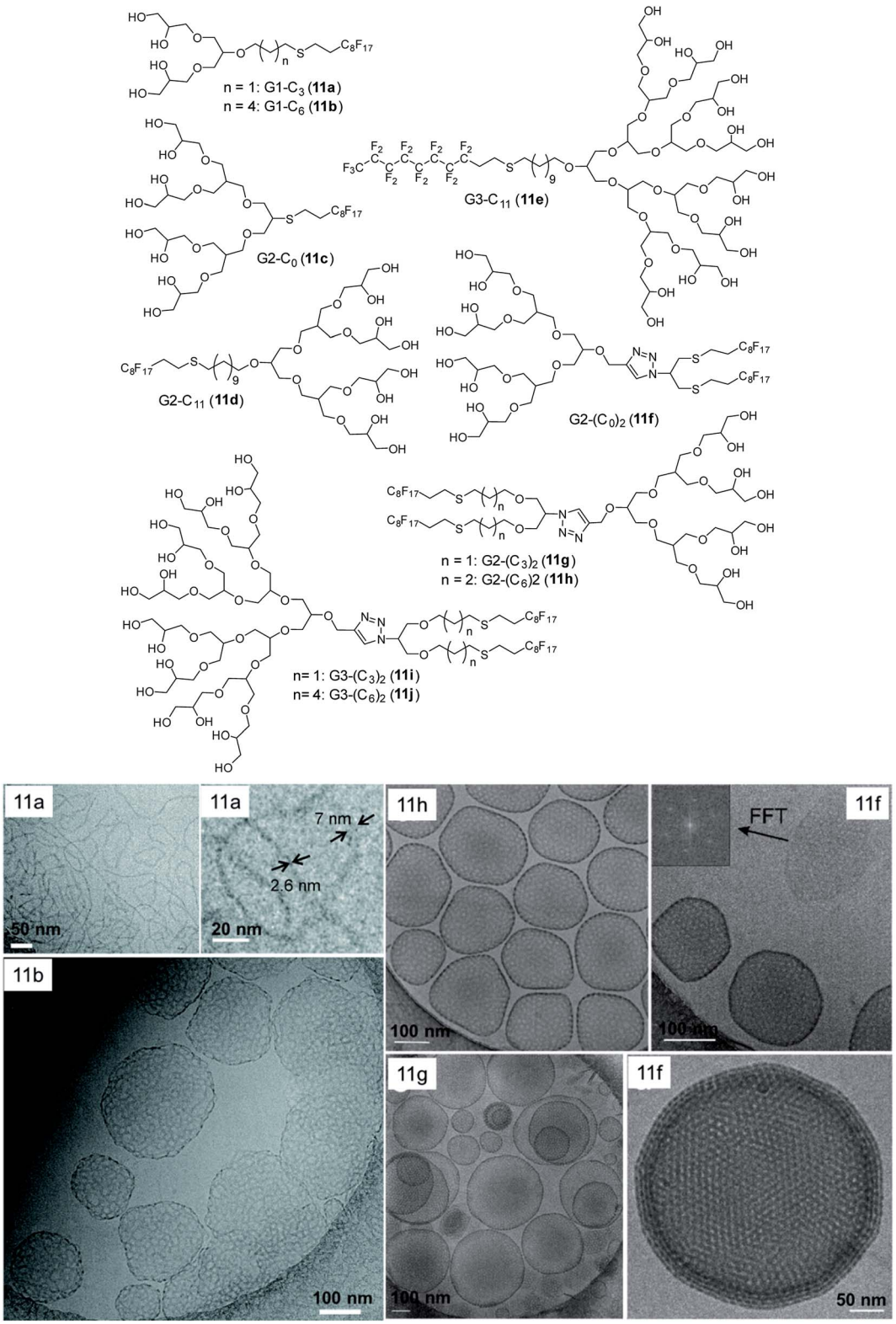

Fig. 20 Molecular structures of dendronized amphiphiles with fluorinated chains (**11a–11j**) and cryo-TEM images of different self-assembled structures obtained from these fluorinated dendron structures including stomatosomes with double diamond network in **11g**. Adapted from ref. 67. Copyright 2018 Royal Society of Chemistry.

Trappmann *et al.* reported a family of non-ionic PG dendron based amphiphiles (**9a–9g**) and their assembly into different nanostructures at very low CMC.[65] All the amphiphiles were composed of varying generation of dendron (G1 to G3) linked to different hydrophobic chain (C_{11} or C_{16}) through mono- or bi-aromatic spacer (Fig. 18). It was observed that the size and

morphology of the supramolecular assemblies was depended on the type of a polar head group and hydrophobic alkyl chain. For example, G1 amphiphiles assembled into different morphologies such as ring-like and fiber-like structures, while G2 and G3 amphiphiles formed uniform spherical micelles. One of the important outcomes of this study was preparation of the self-assembled structures that contained as little as 15 molecules and had up to 74% of empty space. This is completely different from the classical SDS surfactant micelles, where majority of core volume is filled by hydrophobic tails. All the amphiphiles were studied for their encapsulation potential using model hydrophobic dyes nile red and pyrene, and it was found that the purely aromatic pyrene dye solubilized in higher extent than the heterocyclic nile red dye. No change in size was observed after encapsulation of dyes, which indicated that the supramolecular assemblies had enough space in the hydrophobic core to accommodate guest molecules without alteration of overall assembly.

By changing the structural parameters of non-ionic dendritic amphiphiles, various self-assembled nanostructures were engineered by Thota *et al.*[66] They found that in case of G2 amphiphiles (**10a–10c**), shape played a major role compared to HLB value and distinct morphologies resulted on fine tuning the structural parameters. Symmetric G2 amphiphiles (**10a** and **10c**) showed morphological transition from worm-like micellar structure to vesicles, depending upon the chain length of lipophilic part (Fig. 19). On the other hand, unsymmetrical G2 amphiphile led to the formation of spherical and worm-like micelles. The co-existence of two types of self-assembly was also supported by bimodal distribution in DLS. Moreover, all the G3 amphiphiles (**10d–10f**) showed the presence of monodisperse micelles of diameter less than 10 nm, irrespective of the structure of the lipophilic part, which was in good agreement with DLS data. They were further investigated for the encapsulation of nile red and nimodipine, and defined morphology was observed even after the encapsulation of guest molecules.

In another study, the morphology of similar type of fluorinated dendritic amphiphiles was investigated, in which the curvature of the single molecule determined the shape of self-assembled aggregates.[67] In contrast to simple alkyl chain, fluorinated chain gives extra stiffness favouring planar architecture. All G3 amphiphiles irrespective of the number of perfluoro chain as well as single-tailed G2 amphiphiles, self-assembled into spherical micelles (Fig. 20). In these amphiphiles, bulky G3 or G2 dendron overcame the hydrophobic effect of perfluoro chain and dictated the self-assembly of these compounds into small spherical micelles. When the size of the head group was decreased to G1, the morphology changed, and G1-C_3-R_f formed ribbon like structure. However, G1 with longer spacer *i.e.* (G1-C_6-R_f) resulted in highly branched vesicle-like structures with high contrast rims. The most remarkable structure reporte in this study were stomatosomes, perforated vesicles which were observed in the case of double-tail G2 amphiphiles *i.e.* **11f** (G2-$(C_0)_2$), **11g** (G2-$(C_3)_2$), **11h** (G2-$(C_6)_2$ in Fig. 17B) with two tails of different spacer lengths (C_0 to C_6). Interestingly, these stomatostomes were metastable and transformed into a bi-continuous cubic network with double diamond symmetry (Fig. 20, **11g**).

To explore the impact of chirality on the supramolecular assembly, dendronized amphiphiles with the chiral head group have been studied by Kumar *et al.*[68] Enantiomeric amphiphiles (**12a–12b**, Fig. 21) were prepared and compared to their meso-form achiral analogue (**12c**). The study showed that not only hydrophilic-hydrophobic balance, but also the spatial arrangement of architectures was important to achieve well-defined self-assembled nanostructures. Structurally, all the studied amphiphiles possessed PG G1 dendron linked to a single long hydrophobic alkyl chain through the aromatic spacer. Both chiral enantiomers assembled into twisted ribbon like structures, in which the right-handedness and left-handedness were observed for *S*,*S*-G1 and *R*,*R*-G1 respectively (Fig. 21). Intermolecular H-bonding of 1°-OH and 2°-OH groups of isomers seemed to be responsible for the twisted configuration of the self-assembled structures. Interestingly, the *meso*-isomers aggregated into uniform disk-like and elongated cylindrical assemblies, whereas the racemic mixture formed planar platelets with length ranging from few nm to micrometers, but without a chiral ultrastructure.

In addition to these interesting structures, which can be controlled by initial chirality of the amphiphiles, control over

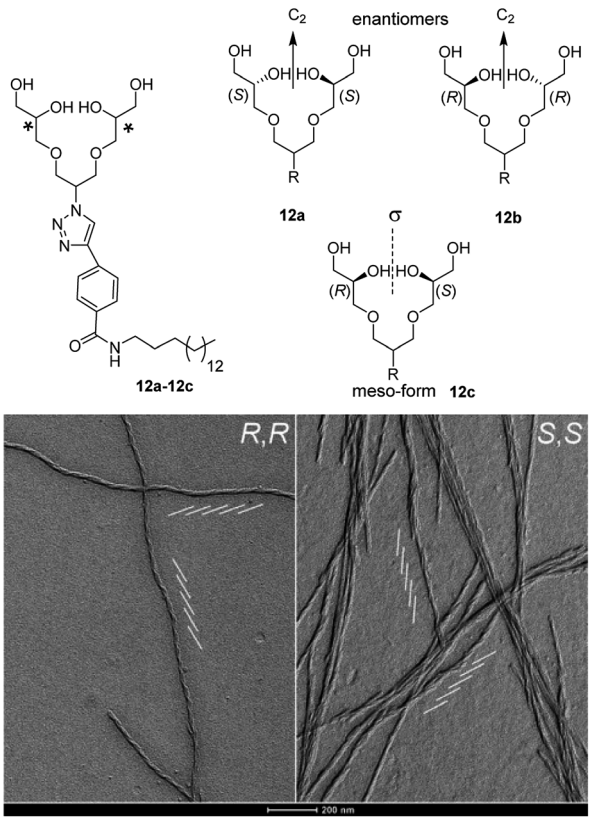

Fig. 21 Chiral and non-chiral dendron amphiphiles(**12a–12c**), and the cryo-TEM images (after 24 h of gel preparation) of their self-assembled structures. A network of twisted ribbons with left-handedness for *R*,*R*-G1 and right-handedness for *S*,*S*-G1 were observed. Parallel oblique white lines show the directions of the twist. Adapted with permission from ref. 68. Copyright 2016 Wiley-VCH Verlag GmbH & Co. KGaA.

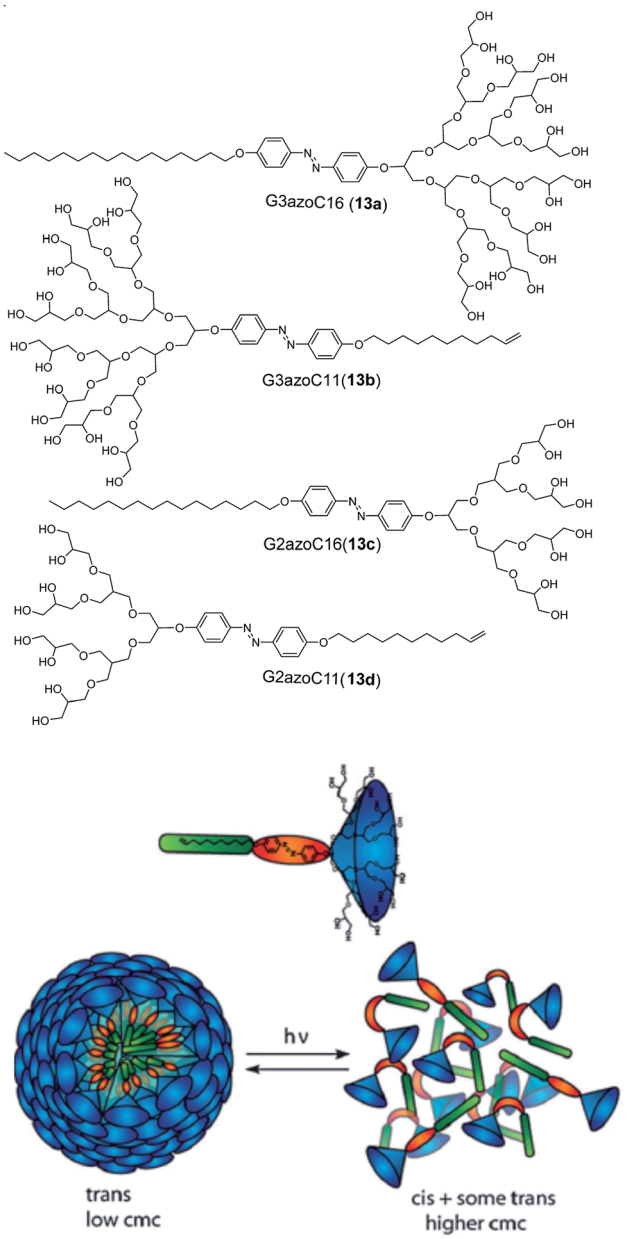

Fig. 22 Molecular structures of dendron amphiphiles (13a–13d) containing azo-benzene and proposed disruption of aggregates by light through *trans–cis* isomerization. Reprinted from ref. 69. Copyright 2011 Royal Society of Chemistry.

the self-assembly can be achieved by design of photo-responsive dendron amphiphiles with the help of azobenzene (Fig. 22).[69] Within these systems, CMC can be modified by UV-light which impacts *cis*–trans isomerization (see also Fig. 12) and results in switchable structures. The size of the micelles formed by these amphiphiles was found to be related to photo stationary state (*i.e.* equilibrium chemical composition under UV light), where smaller micelles displayed higher photo stationary state in comparison to the larger sized ones. The comparison of these amphiphiles with the amphiphile containing *m*PEG-500 (chosen because of similar molecular weight of *m*PEG-500 and G2 dendron) instead of PG dendron, showed that all four dendron-based amphiphiles self-assembled into definite micelles. The *cis–trans* isomerization of dendron amphiphiles also proceeded more readily than in the case of the linear *m*PEG amphiphile, which assembled into ill-defined aggregates. The CMC of the *m*PEG amphiphile was also not affected by UV irradiation, possibly because the linear geometry of PEG led to highly dense packing of the micelles and thus, the steric crowding restricted the isomerization. In order to illustrate the effect of photo-switching in azo-benzene aggregates, solubilization of model dye nile red was undertaken. The results revealed that upon photo irradiation, the CMC of the aggregate increased together with light attenuated uptake of nile red. Furthermore, the solubilization of model dye nile red used to illustrate the effect of photo-switching in azo-benzene aggregates showed an increase in CMC after photo irradiation, together with light attenuated uptake of nile red.

A significant challenge of drug delivery is the low solubility of many important drugs, in particular those used in chemotherapy. Dendon based amphiphiles (**14a–14e**, Fig. 23) can be used to increase the aqueous stability and solubility of such insoluble drugs, as has been shown in the case of the anticancer

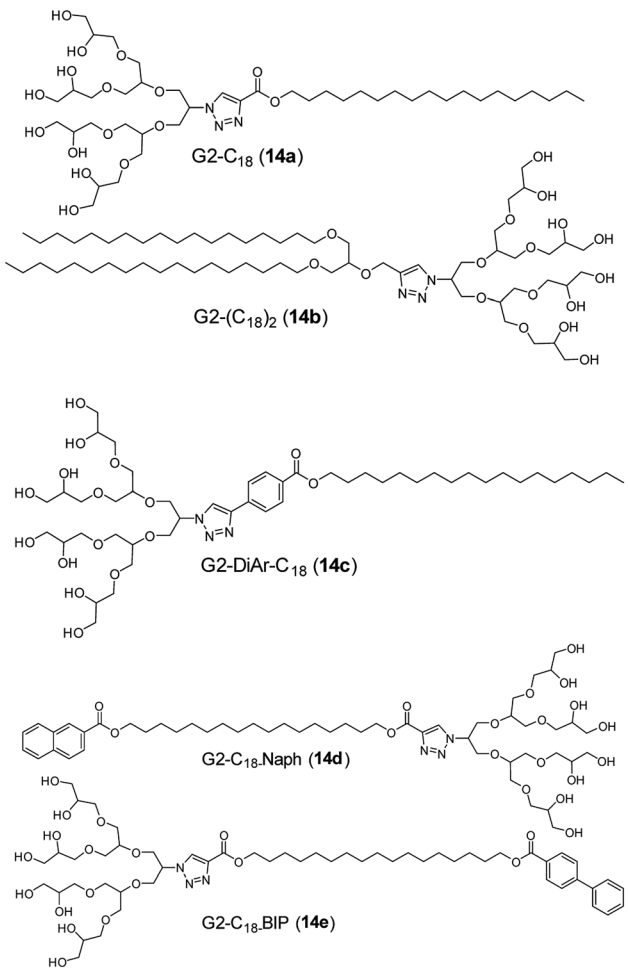

Fig. 23 Molecular structures of dendrone amphiphiles (14a–14e) used for formulation of insoluble chemotherapeutics.

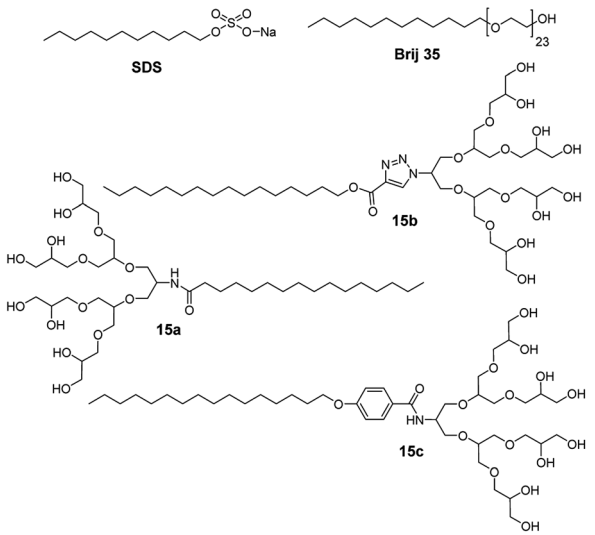

Fig. 24 Molecular structures of amphiphiles **15a–15c**, including commercial SDS and Brij 35 used for interaction and purification of carbon nanotubes.

drug Sagopilone.[70] The effect of different hydrophobic tail structures on the solubilization of the drug, formulation stability profile and cytotoxicity was studied and compared with standard excipients such as Cremophor® ELP and polysorbate 80. Structurally, all the compounds contained G2 dendron attached to various hydrophobic C_{18} chains. All the compounds self-assembled into small monodisperse micelles of size in the range of 7–10 nm, with the exception of G2-$(C_{18})_2$ amphiphile. These amphiphiles exhibited 2–3 fold higher drug solubilization in comparison to standards tested, with the di-aromatic spacer G2-DiAr-C_{18} (**14c**) showing the best results. Such remarkable solubilization increase together with the outstanding formulation stability proved that carefully designed dendron structures can be used a suitable alternative to solubilizing excipients and building blocks for design of efficient drug nanocarriers.

Interestingly, PG based amphiphiles were also shown to be useful to increase the dispersion of the carbon nanotubes (CNT) in water.[71–73] The replacement of a sulphate group of SDS with PG dendron produced compounds which could be used for purification and de-bundling of single walled CNT (SWCNT) at low concentrations. Such an ability is a result of the steric hindrance and inter/intramolecular H-bonding provided by the dendron. Furthermore, the incorporation of extra aromatic moiety between PG head group and a hydrophobic tail increased the amphiphile's selectivity towards SWCNTs. Interestingly, depending on the type of amphiphile, nanotubes of different chirality could be found in the suspension. It should be noted that the electronic and optical of CNTs depend on the chirality of nanotubes. Thus, having the ability to isolate CNTs of different chirality is of huge interest particularly for electronic applications.

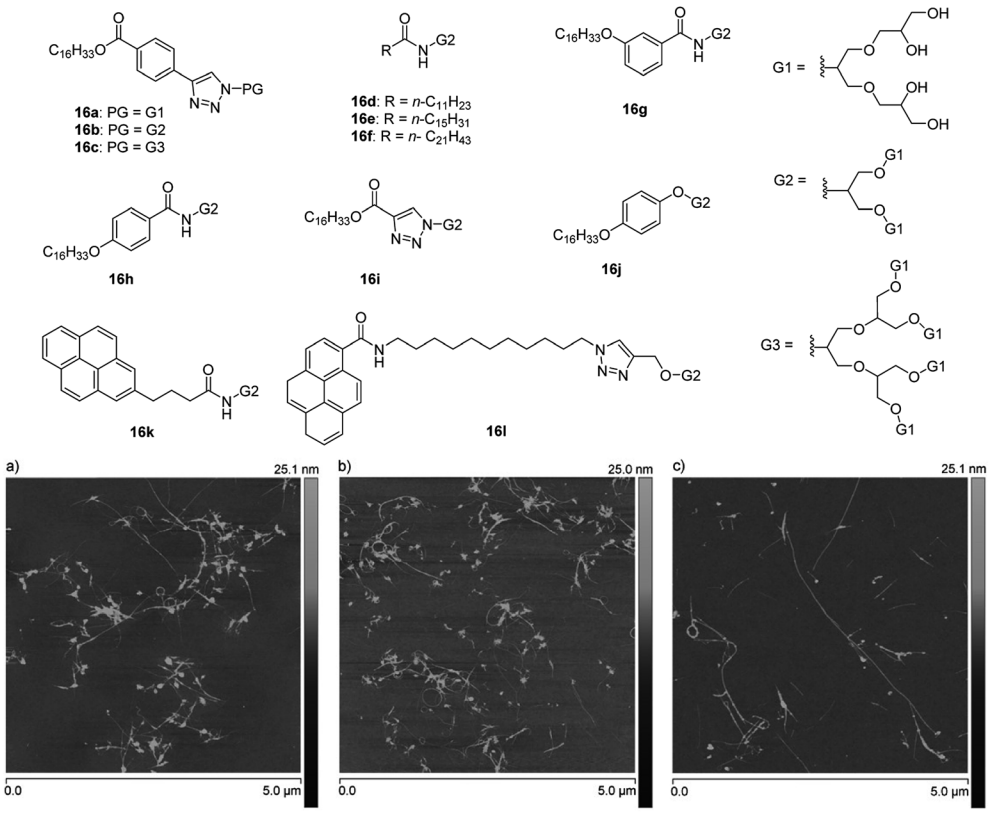

Fig. 25 Molecular structures of amphiphiles **16a–16l** used for isolation and solubilization of CNTs and AFM images of SWNTs dispersed by amphiphiles **16b** (a), **16f** (b), and **16k** (c). Adapted with permission from ref. 75. Copyright 2016 Wiley-VCH Verlag GmbH & Co. KGaA.

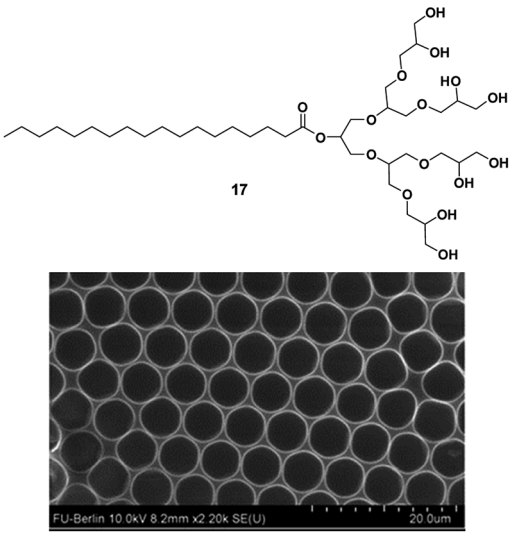

Fig. 26 Molecular structure of amphiphile **17** used in design of the porous structures and SEM micrographs of surface prepared from a mixture of polystyrene and amphiphile **17** in $CHCl_3$ under high humidity. Adapted with permission from ref. 76. Copyright 2015 Elsevier.

It was also observed that the interaction between the absorbed amphiphile and a nanotube alters the properties of nanotubes. Bluemmel *et al.* studied the replacement of absorbed amphiphile **15a** on CNT surface by other amphiphiles (**15b** and **15c**), and explored the effect of different aromatic spacers (Fig. 24).[74] The amphiphile consisting of aromatic phenyl ring spacer (**15c**) displayed higher replacement of starting alkyl chain amphiphile, thus, indicating an enhanced interaction with CNT. On the other hand, amphiphiles composed of triazolyl ring spacer (**15b**) showed negligible replacement and hence, suggesting a weaker interaction with CNT. Thus, the chiral distribution inside the sample could be controlled by selection of the amphiphilic surfactant.

SWCNTs were isolated and solubilized also using a similar series of amphiphiles (**16a–16l**, Fig. 25) derived by the variation of PG dendron generation and hydrophobic tails.[75] The study correlated the hydrophobicity of the amphiphiles, which was controlled by varying the tail size from C_{12} to C_{22}, with their ability to break up the aggregation of SWCNTs. The amphiphiles exhibiting longer chain length displayed improved exfoliation ability. On the other hand, the size and composition of the head group was found to only weakly impact the suspension behavior, whereas the configuration of linkage between head and tail seemed to play an important role. *Meta* (**16g**) and *para*-isomers (**16h**) of benzamide-based amphiphiles showed a remarkable difference in solubilization behavior, where *meta*-isomer exhibited higher stability and lower aggregation/bundleness of nanotube in comparison to *para*-isomer. Overall, amphiphiles consisting of flexible and bent shaped linker displayed were more effective in purification and solubilization of CNTs, which were further illustrated by using statistical AFM analysis of isolated CNTs.

Another interesting structural property of functional materials is porosity, which cannot be easily introduced to the material systems. In order to develop highly porous surface, dendritic amphiphiles having different functionality were employed as additives in binary blend during breath figure technique.[76] Breath-figure self-assembly is a self-assembly phenomenon where honeycomb micro-scaled polymer patterns are formed by the condensation of water droplets.

Table 1 PEG-based nanocarriers in clinical trials for anticancer therapy. Adapted from ref. 79. Copyright 2019 With permission from the Royal Society of Chemistry

Nanocarrier	Trade name	Drug	Disease	Clinical trial phase
PEG-drug conjugate	Prothecan	Camptothecin (with glycine linker)	Gastric and gastroesophageal tumors	II
	EZN-2208	SN38 (camptothecin analog)	Metastatic breast tumor	II
	NKTR-102	Irinotecan	Second line colorectal tumor Metastatic breast tumor Platinum-resistant ovarian Tumor and metastatic cervical tumor	II
PEG-based polymeric micelle	NK911	Doxorubicin	Pancreatic tumor	I
	NK105	Paclitaxel	Advanced stomach tumor	II
	NC-6004	Cisplatin	Solid tumors	I/II
	Genexol® PM	Paclitaxel	Breast tumor	IV
			Pancreatic tumor	II
			Non-small-cell lung tumor in combination with carboplatin	II
			Pancreatic tumor in combination with gemcitabine	I/II
			Ovarian tumor in combination with carboplatin	I/II
PEG-based polymeric liposome	Doxil®/ Caelyx®	Doxorubicin	Breast tumor, ovarian tumor, multiple myeloma, Kaposi's sarcoma	Approved
	Thermodox®	Doxorubicin	Liver tumor, breast tumor	III
	Lipoplatin	Cisplatin	NSCLC, breast tumor, gastric tumor	III
	SPI-77	Cisplatin	Ovarian tumor	II

"Breath-figure" relates to fog formation that occurs when water vapor contacts a cold surface. Here, evaporation of volatile polymer solution in a humid atmosphere results in decrease of solution surface temperature, thus causing condensation of water as small droplets on the surface. The formed droplets can grow and be ordered in a honeycomb structure, resulting in a porous polymeric film after complete solvent and water evaporation. The morphology and distribution of the pores obtained are governed by factors such as humidity, temperature, polymer concentration, as well as the topological and functional characteristics of the polymer employed. The effect of chemical structure and hydrophilicity of the amphiphiles together with blend composition were studied to create wide variety of surfaces. The G2 dendronized amphiphile **17** (Fig. 26) stabilized the condensed water droplets was found to be a superior additive for the production of well-ordered honeycomb-like patterned surfaces when compared to commercial Brij L4 surfactant. Thus, surface with tunable pore size varying from 5 to 14 μm could be fabricated by use of highly defined, low molecular weight and monodispersed amphiphilic nanostructures. Moreover, the high water solubility of the amphiphiles eased their removal after the formation of the porous structure, thus, offering the possibility of reuse.

Conclusions

In this review we have presented an overview of the supramolecular assemblies formed by non-ionic small amphiphiles in aqueous medium. Beyond the formation of well-known spherical micelles and vesicles, amphiphilic architectures can self-assemble into more ordered high aspect ratio assemblies such as fibers, helices, ribbons, and tubes, as driven by the hydrophobic and other non-covalent structure directing interactions. The fine tuning of the aggregate size and morphology is crucial for their application in nanotechnology and materials chemistry, and this was achieved by changing the molecular structure of the amphiphilic architecture (type of the hydrophilic and hydrophobic segments, stereochemistry, and so forth) and by use of the external stimuli (light and enzyme activity). Responsive self-assembled structures are particularly interesting from the point of drug release and design of adaptable materials, and it could be expected that further work in the realm of amphiphiles will focus on introduction of functional groups that enable such control. Amphiphiles will continue playing an important role in deciphering the self-assembly, and as we learn more about complex architectures, we will be able to design more efficient and controllable drug delivery and molecular storage systems. In addition, due to their versatility and scalability, amphiphiles have huge potential to be employed in preparation and purification of other nanostructures as demonstrated in a case of carbon nanotubes or porous nanostructure design.

Challenges and future perspective

The addition of PEG to pharmaceutical formulations has several advantages such as increased water solubility and renal clearance, high chemical stability, decreased interaction with blood components and improved biocompatibility, thus, PEG is currently is most used material approved for applications in drug delivery. However, research over past few years has shown that it also comes with some drawbacks such as possible degradation under stress, anti-PEG antibody formation, PEG-associated cytoplasmic vacuolation and accumulation in body.[77] Polyglycerols have emerged as potential alternative to PEG but there are still insufficient studies related to their degradation under stress, interaction with immune system and accumulation behavior. Small amphiphiles discussed in this review require extensive studies in terms of above mentioned parameters as well as more advanced 3D cell studies prior to *in vivo* exploration. The realm of biology is immensely complex and more work is needed to create 'smart' multi-stimuli-responsive architectures for successful bioapplications, where self-assembly can be directed by various stimuli such as temperature, pH, light or ions. Learning from nature and looking into bioinspired self-assembly strategies in combination with chemical cross-linking could help us prepare larger amounts of stable structures which could be loaded with desired drugs. In terms of the translation from the lab to the clinic, no non-ionic small amphiphile is approved yet but several PEGylated polymeric systems and drug-conjugates have made it through clinical trials to treat cancer.[78] For example PEG-block-poly(D,L-lactide) polymeric micelle-formulated Paclitaxel (Genexol® PM) and PEGylated-SN38 (EZN-2208) are in clinical trials and PEGylated liposomal doxorubicin (Doxil) is clinically approved for treatment of various cancers (Table 1).[78,79] With further development of biomarkers for particular diseased cells, and with design advances, we anticipate small non-ionic amphiphiles will play a huge role not only in drug delivery but as a building block in tissue engineering.

Conflicts of interest

There are no conflicts to declare.

Acknowledgements

B. P. is funded by Cancer research UK Primer Award (C67674/A27887). We acknowledge UGC-CSIR, New Delhi, for providing fellowship to A. M.

References

1 C. Branden and J. Tooze, *Introduction to Protein Structure*., Garland Publishing Inc., New York, 2nd edn, 1999.
2 M. Lee, B.-K. Cho and W.-C. Zin, *Chem. Rev.*, 2001, **101**, 3869–3892.
3 V. Percec, A. E. Dulcey, V. S. K. Balagurusamy, Y. Miura, J. Smidrkal, M. Peterca, S. Nummelin, U. Edlund, S. D. Hudson, P. A. Heiney, H. Duan, S. N. Magonov and S. A. Vinogradov, *Nature*, 2004, **430**, 764–768.
4 M. A. Alam, Y.-S. Kim, S. Ogawa, A. Tsuda, N. Ishii and T. Aida, *Angew. Chem., Int. Ed.*, 2008, **47**, 2070–2073.

5 J. A. A. W. Elemans, A. E. Rowan and R. J. M. Nolte, *J. Mater. Chem.*, 2003, **13**, 2661–2670.
6 F. Reinitzer, *Liq. Cryst.*, 1989, **5**, 7–18.
7 G. M. Whitesides and M. Boncheva, *Proc. Natl. Acad. Sci. U.S.A.*, 2002, **99**, 4769–4774.
8 Y. Liu, B. Liu and Z. Nie, *Nano Today*, 2015, **10**, 278–300.
9 G. S. Hartley, *Aqueous Solutions of Paraffinic-Chain Salts. A Study of Micelle Formation*, Herman, Paris, 1936.
10 M. Ramanathan, L. K. Shrestha, T. Mori, Q. Ji, J. P. Hill and K. Ariga, *Phys. Chem. Chem. Phys.*, 2013, **15**, 10580–10611.
11 A. Sorrenti, O. Illa and R. M. Ortuño, *Chem. Soc. Rev.*, 2013, **42**, 8200–8219.
12 X. Zhang and C. Wang, *Chem. Soc. Rev.*, 2011, **40**, 94–101.
13 S. Gupta, R. Tyagi, V. S. Parmar, S. K. Sharma and R. Haag, *Polymer*, 2012, **53**, 3053–3078; A. Barnard, M. Calderon, A. Tschiche, R. Haag and D. K. Smith, *Org. Biomol. Chem.*, 2012, **10**, 8403–8409.
14 N. J. Butcher, G. M. Mortimer and R. F. Minchin, *Nat. Nanotechnol.*, 2016, **11**, 310–311.
15 S. Gupta, R. Tyagi, V. S. Parmar, S. K. Sharma and R. Haag, *Polymer*, 2012, **53**, 3053–3078.
16 I. N. Kurniasih, H. Liang, S. Kumar, A. Mohr, S. K. Sharma, J. P. Rabe and R. Haag, *J. Mater. Chem. B*, 2013, **1**, 3569–3577.
17 B. M. Rosen, C. J. Wilson, D. A. Wilson, M. Peterca, M. R. Imam and V. Percec, *Chem. Rev.*, 2009, **109**, 6275–6540.
18 B. N. S. Thota, L. H. Urner and R. Haag, *Chem. Rev.*, 2016, **116**, 2079–2102.
19 A. Kumar, A. Khan, S. Malhotra, R. Mosurkal, A. Dhawan, M. K. Pandey, B. K. Singh, R. Kumar, A. K. Prasad, S. K. Sharma, L. A. Samuelson, A. L. Cholli, C. Len, N. G. J. Richards, J. Kumar, R. Haag, A. C. Watterson and V. S. Parmar, *Chem. Soc. Rev.*, 2016, **45**, 6855–6887.
20 A. Khan, S. K. Sharma, A. Kumar, A. C. Watterson, J. Kumar and V. S. Parmar, *ChemSusChem*, 2014, **7**, 379–390.
21 X. Cui, S. Mao, M. Liu, H. Yuan and Y. Du, *Langmuir*, 2008, **24**, 10771–10775.
22 J. N. Israelachvili, *Intermolecular and Surface Forces*, Academic Press, New York, USA, 2nd edn, 1992.
23 J. N. Israelachvili, D. J. Mitchell and B. W. Ninham, *J. Chem. Soc. Faraday Trans. II*, 1976, **172**, 1525–1568.
24 J. H. Fendler, *Membrane Mimetic Chemistry*, Wiley, New York, 1983.
25 R. Langer, *Science*, 1990, **249**, 1527–1533.
26 A. Memoli, L. G. Palermiti, V. Travagli and F. Alhaique, *J. Soc. Cosmet. Chem.*, 1993, **44**, 123–128.
27 A. Memoli, L. G. Palermiti, V. Travagli and F. Alhaique, *J. Soc. Cosmet. Chem.*, 1994, **45**, 167–172.
28 G. Gregoriadis, *Trends Biotechnol.*, 1995, **13**, 527–537.
29 I. F. Uchegbu and S. P. Vyas, *Int. J. Pharm.*, 1998, **172**, 33–70.
30 D. E. Discher and A. Eisenberg, *Science*, 2002, **297**, 967–973.
31 Y. Barenholz, *J. Controlled Release*, 2012, **160**, 117–134.
32 L. C. Palmer and S. I. Stupp, *Acc. Chem. Res.*, 2008, **41**, 1674–1684.
33 A. Brizard, C. Aimé, T. Labrot, I. Huc, D. Berthier, F. Artzner, B. Desbat and R. Oda, *J. Am. Chem. Soc.*, 2007, **129**, 3754–3762.
34 Y. Kim, W. Li, S. Shin and M. Lee, *Acc. Chem. Res.*, 2013, **46**, 2888–2897.
35 F. Liu, H. Qi, L. Huang and D. Liu, *Gene Ther.*, 1997, **4**, 517–523.
36 J. P. Yang and L. Huang, *Gene Ther.*, 1997, **4**, 950–960.
37 O. Zelphati, L. S. Uyechi, L. G. Barron and F. C. Szoka, *Biochim. Biophys. Acta Lipids Lipid. Metabol.*, 1998, **1390**, 119–133.
38 P. P. Karmali and A. Chaudhuri, *Med. Res. Rev.*, 2007, **27**, 696–722.
39 M. E. N. P. Ribeiro, C. L. de Moura, M. G. S. Vieira, N. V. Gramosa, C. Chaibundit, M. C. de Mattos, D. Attwood, S. G. Yeates, S. K. Nixon and N. M. P. S. Ricardo, *Int. J. Pharm.*, 2012, **436**, 631–635.
40 R. M. Fuoss and D. Edelson, *J. Am. Chem. Soc.*, 1951, **73**, 269–273.
41 J.-H. Fuhrhop and J. Mathieu, *Angew. Chem., Int. Ed. Engl.*, 1984, **23**, 100–113.
42 Y. Yan, T. Lu and J. Huang, *J. Colloid Interface Sci.*, 2009, **337**, 1–10.
43 S. Prasad, K. Achazi, B. Schade, R. Haag and S. K. Sharma, *Eur. Polym. J.*, 2018, **109**, 506–522.
44 R. Rashmi, A. K. Singh, K. Achazi, B. Schade, C. Böttcher, R. Haag and S. K. Sharma, *RSC Adv.*, 2018, **8**, 31777–31782.
45 M. Wyszogrodzka, K. Möws, S. Kamlage, J. Wodzińska, B. Plietker and R. Haag, *Eur. J. Org Chem.*, 2008, **2008**, 53–63.
46 M. Wyszogrodzka and R. Haag, *Chem.–Eur J.*, 2008, **14**, 9202–9214.
47 L. H. Urner, M. Schulze, K. Folmert, R. Haag and K. Pagel, *ChemPhysChem*, 2019, **20**, 1690–1697.
48 L. H. Urner, B. N. S. Thota, O. Nachtigall, S. Warnke, G. von Helden, R. Haag and K. Pagel, *Chem. Commun.*, 2015, **51**, 8801–8804.
49 A. Bunton, L. Robinson, J. Schaak and M. F. Stam, *J. Org. Chem.*, 1971, **36**, 2346–2350.
50 F. Devínsky, I. Lacko, F. Bittererová and L. Tomečková, *J. Colloid Interface Sci.*, 1986, **114**, 314–322.
51 Y.-p. Zhu, A. Masuyama and M. Okahara, *J. Am. Oil Chem. Soc.*, 1990, **67**, 459–463.
52 F. M. Menger and C. A. Littau, *J. Am. Chem. Soc.*, 1991, **113**, 1451–1452.
53 F. Bordi, G. Cerichelli, N. D. Berardinis, M. Diociaiuti, L. Giansanti, G. Mancini and S. Sennato, *Langmuir*, 2010, **26**, 6177–6183.
54 L. Shi, F. Chen, N. Sun and L. Zheng, *Soft Matter*, 2015, **11**, 4075–4080.
55 G. Wang, Y. Kang, B. Tang and X. Zhang, *Langmuir*, 2015, **31**, 120–124.
56 W. Zhao and Y. Wang, *Adv. Colloid Interface Sci.*, 2017, **239**, 199–212.
57 R. S. G. Krishnan, S. Thennarasu and A. B. Mandal, *J. Phys. Chem. B*, 2004, **108**, 8806–8816.
58 A. K. Singh, B. N. S. Thota, B. Schade, K. Achazi, A. Khan, C. Böttcher, S. K. Sharma and R. Haag, *Chem.–Asian J.*, 2017, **12**, 1796–1806.
59 S. Prasad, K. Achazi, C. Böttcher, R. Haag and S. K. Sharma, *RSC Adv.*, 2017, **7**, 22121–22132.

60 P. Manchanda, K. Achazi, D. Verma, C. Böttcher, R. Haag and S. K. Sharma, *Polymers*, 2020, **12**, 1421.
61 B. Parshad, P. Yadav, Y. Kerkhoff, A. Mittal, K. Achazi, R. Haag and S. K. Sharma, *New J. Chem.*, 2019, **43**, 11984–11993.
62 R. Rashmi, F. Zabihi, A. K. Singh, K. Achazi, B. Schade, S. Hedtrich, R. Haag and S. K. Sharma, *Int. J. Pharm.*, 2020, **580**, 119212.
63 S. Prasad, K. Achazi, B. Schade, R. Haag and S. K. Sharma, *Macromol. Biosci.*, 2018, **18**, 1800019.
64 A. Mittal, A. K. Singh, A. Kumar, Parmanand, K. Achazi, R. Haag and S. K. Sharma, *Polym. Adv. Technol.*, 2020, **31**, 1208–1217.
65 B. Trappmann, K. Ludwig, M. R. Radowski, A. Shukla, A. Mohr, H. Rehage, C. Böttcher and R. Haag, *J. Am. Chem. Soc.*, 2010, **132**, 11119–11124.
66 B. N. S. Thota, H. v. Berlepsch, C. Böttcher and R. Haag, *Chem. Commun.*, 2015, **51**, 8648–8651.
67 H. v. Berlepsch, B. N. S. Thota, M. Wyszogrodzka, S. de Carlo, R. Haag and C. Böttcher, *Soft Matter*, 2018, **14**, 5256–5269.
68 S. Kumar, K. Ludwig, B. Schade, H. von Berlepsch, I. Papp, R. Tyagi, M. Gulia, R. Haag and C. Böttcher, *Chem.–Eur J.*, 2016, **22**, 5629–5636.
69 C. Kördel, C. S. Popeney and R. Haag, *Chem. Commun.*, 2011, **47**, 6584–6586.
70 A. Richter, A. Wiedekind, M. Krause, T. Kissel, R. Haag and C. Olbrich, *Eur. J. Pharm. Sci.*, 2010, **40**, 48–55.
71 A. Setaro, C. S. Popeney, B. Trappmann, V. Datsyuk, R. Haag and S. Reich, *Chem. Phys. Lett.*, 2010, **493**, 147–150.
72 A. Setaro, C. S. Popeney, M. U. Witt, P. Bluemmel, M. Glaeske, R. Haag and S. Reich, *Phys. Status Solidi B*, 2015, **252**, 2536–2540.
73 A. Setaro, C. S. Popeney, B. Trappmann, R. Haag and S. Reich, *Phys. Status Solidi B*, 2010, **247**, 2758–2761.
74 P. Bluemmel, A. Setaro, C. S. Popeney, B. Trappmann, R. Haag and S. Reich, *Phys. Status Solidi B*, 2011, **248**, 2532–2535.
75 C. S. Popeney, A. Setaro, R.-C. Mutihac, P. Bluemmel, B. Trappmann, J. Vonneman, S. Reich and R. Haag, *ChemPhysChem*, 2012, **13**, 203–211.
76 A. S. De León, S. Malhotra, M. Molina, R. Haag, M. Calderón, J. Rodríguez-Hernández and A. Muñoz-Bonilla, *J. Colloid Interface Sci.*, 2015, **440**, 263–271.
77 K. Knop, R. Hoogenboom, D. Fischer and U. S. Schubert, *Angew. Chem., Int. Ed.*, 2010, **49**, 6288–6308.
78 P. Mishra, B. Nayak and R. K. Dey, *Asian J. Pharm. Sci.*, 2016, **11**, 337–348.
79 S. Parveen, F. Arjmand and S. Tabassum, *RSC Adv.*, 2019, **9**, 24699–24721.